Okhotsk Sea and Polar Oceans Research 2 (2018) 7-12

Article

Comparison of the Arctic tropospheric structures from the ERA-Interim reanalysis with in situ observations

Jun INOUE[1], Kazutoshi SATO[2] and Kazuhiro OSHIMA[3]

[1]*National Institute of Polar Research, Tachikawa, Japan*
[2]*Antarctic Climate & Ecosystems Cooperative Research Centre, Tasmania, Australia*
[3]*Japan Agency for Marine-Earth Science and Technology, Yokosuka, Japan*

(Received August 29, 2017; Revised manuscript accepted January 12, 2018)

Abstract

Using data sets of frequent radiosonde observations and surface meteorological observations obtained during an Arctic cruise in September 2014, the reproducibility of the ERA-Interim reanalysis product was evaluated with reference to the upper troposphere. Relative humidity in the ERA-Interim reanalysis was found overestimated with a positive bias of cloud cover in the upper troposphere, which was attributable partly to the parameterization of cloud formation. Relative humidity in the lower stratosphere was also higher than observed, suggesting that a small amount of moisture was transported from the troposphere to the stratosphere via mixing induced by radiative/evaporative cooling at the level of the excessive upper cloud. Ozone profiles, based on ozonesonde observations, revealed that a positive bias of ozone partial pressure below the tropopause in the ERA-Interim reanalysis could be attributed to downward transport of ozone from the lower stratosphere into the upper troposphere via entrainment of a high-ozone air mass. The positive bias of upper cloud in the ERA-Interim reanalysis also affected downward radiation at the surface for the case of absent boundary layer clouds.

Key words: Arctic, reanalysis, cloud, ozone, surface radiation

1. INTRODUCTION

Arctic cloud is one of the most important components of the Arctic climate system for determining surface heat budgets over both the sea ice and the open ocean. However, it is known that the reproducibility of Arctic cloud in climate models is inadequate and that its evaluation is difficult because of the lack of observations for validation purposes (e.g., surface boundary conditions, boundary layer profiles, and aerosol/condensation nuclei). Several special field campaigns and model intercomparison projects have been performed to try to overcome this difficulty and to develop parameterizations related to clouds (e.g., Curry *et al.*, 2000; Uttal *et al.*, 2002; Curry and Lynch, 2002). Cloud-top radiative cooling enhances the vertical mixing of heat, moisture, and momentum in the boundary layer (e.g., Nicholls and Leighton, 1986), but it is a very complicated process and it is hard to observe without aircraft. In addition, multiple layers of cloud in the Arctic, which consist of stable boundary layer clouds near the surface and mid-/upper-layer clouds associated with cyclones, make it difficult to understand the surface heat budget (e.g., Inoue *et al.*, 2005; 2006).

The ERA-Interim reanalysis product (Dee *et al.*, 2002) is known as one of the best reanalysis products for Arctic research (Inoue *et al.*, 2011; Lyndsay *et al.*, 2014), although cloud cover is also reproduced well in other reanalysis products (Liu and Key, 2016). Although lower boundary layer clouds have been investigated and compared with in situ observations

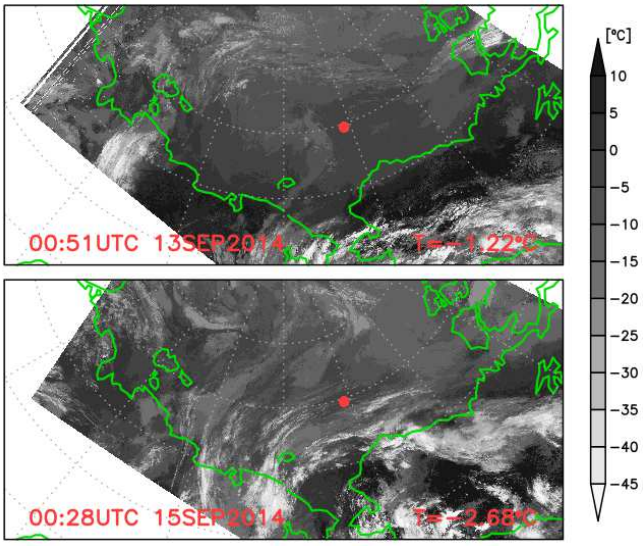

Fig. 1 Infrared satellite images (NOAA/AVHRR) received onboard *RV Mirai* on 13 and 15 September 2014. Red dot indicates location of fixed-point observations. Numeric value in the lower-right corner in each image is the infrared temperature at the fixed point.

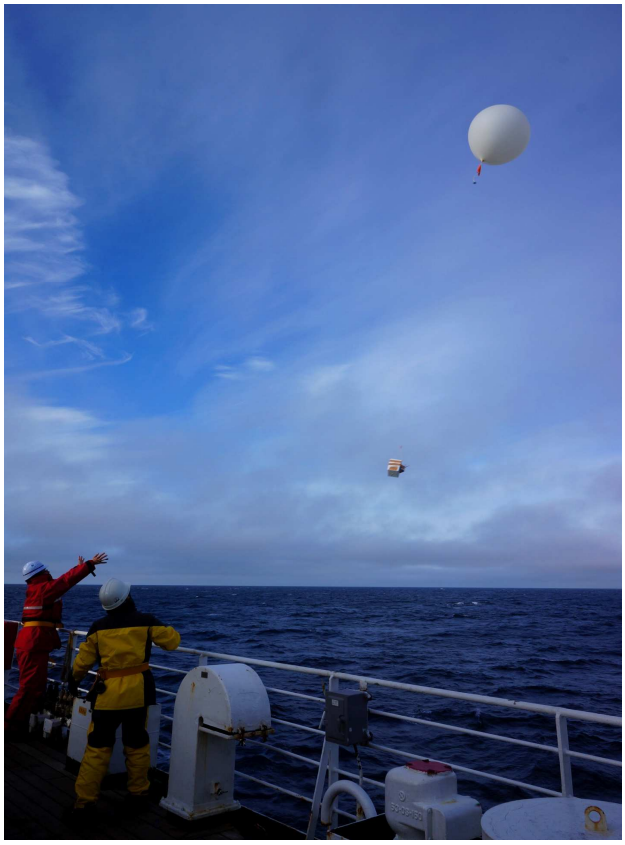

Fig. 2 Launching an ozonesonde from *RV Mirai* at 2200 UTC 14 September 2014.

and model outputs (e.g., Intrieri *et al.*, 2002; Inoue *et al.*, 2006; Schweiger *et al.*, 2008; Tjernström *et al.*, 2008; Sato *et al.*, 2012), the upper-tropospheric situation has not been evaluated fully. Because of Arctic amplification, moisture transport is enhanced, even in the upper troposphere, and vice versa (e.g., Maturilli and Kayser, 2016); thus, validation of the reproducibility at the upper troposphere using observation data is desirable.

In September 2014, as part of an Arctic research cruise undertaken by a Japanese research vessel in the Chukchi Sea, frequent fixed-point radiosonde observations and surface meteorological measurements were acquired. Using these data sets, this study investigated the reproducibility of the ERA-Interim reanalysis product with reference to the upper troposphere and related processes.

2. DATA

2.1 Radiosonde observations obtained during the *RV Mirai* Arctic cruise

In September 2014, two types of special radiosonde observations were performed during an Arctic cruise by *RV Mirai* under sea-ice-free conditions. One comprised regular 3-hourly (0000–2100 UTC) GPS radiosonde observations (RS92-SGPD, Vaisala) acquired above a fixed point in the Chukchi Sea (74.75°N, 162.00°W; red dot in Fig. 1) during 6–25 September 2014. After each observation, all data were sent to the World Meteorological Organization via the Japan Meteorological Agency and the global telecommunication system (GTS).

The other type of observation comprised ozonesonde observations (Fig. 2) acquired using Electrochemical Concentration Cell ozonesondes (6A, Science Pump Corp.), an Ozone Interface Kit (RSA921, Vaisala), and a GPS radiosonde (RS92-SGPD, Vaisala). Prior to launch, the ozone sensor was calibrated using an Electrochemical Concentration Cell Ozonesonde Ozonizer/Test Unit TSC-1 (Science Pump Corp.). Ozonesondes were launched every two days at 2200 UTC during 6–24 September 2014. The data were not sent to the GTS.

Ancillary data sets included surface meteorological observations including downward shortwave and longwave radiation, and satellite imagery acquired from the Advanced Very High Resolution Radiometer and received onboard the ship. For further information, the cruise report (Inoue, 2014) is available online (http://www.godac.jamstec.go.jp/catalog/data/doc_catalog/media/MR14-05_all.pdf).

2.2 ERA-Interim product

The ERA-Interim reanalysis product (Dee *et al.*, 2011) (hereafter, ERA-I) was validated using the sounding data acquired during the *RV Mirai* cruise. The horizontal and temporal resolutions of the product are 0.75° × 0.75° and six hours (0000, 0600, 1200, and 1800 UTC), respectively. The parameters used in this study were air temperature, relative humidity, ozone partial pressure, cloud cover, specific humidity, and surface downward radiation. Grid-point mean values, comprising the averages of the two grids (74.25°N, 162.00°W and 75.00°N, 162.00°W) closest to the fixed sampling point (Fig. 1) were used for comparison with the observed values.

3. RESULT

3.1 Validation of reanalysis

Figure 3 shows the vertical profiles of air temperature obtained from the ozonesonde soundings (2200 UTC) and ERA-I (0000 UTC). Because our 3-hourly regular radiosonde observations were assimilated into the ECMWF operational system (ECMWF, 2014), the vertical structure of air temperature is reproduced very well for each day, except for the minimum temperature near the tropopause. The tropopause height is deviated from 300 to 200 hPa because of the intrusion of upper potential vorticity (e.g., 11 September). In the lower troposphere, clear inversion layers can be observed

on 7, 9, 11, 13, and 17 September, while in ERA-I, the inversion layer is reproduced on 7,13 and 17 September. In the lower stratosphere, the temperature is reproduced well.

The structure of relative humidity (Fig. 4) is very different to that of air temperature. The value in ERA-I is overestimated from 20% to 40%, particularly in the mid- and upper troposphere between 500 and 200 hPa although the relative humidity data by radiosondes were assimilated into the system. The vertical distribution of cloud cover in ERA-I indicates that upper-layer clouds are produced in all cases, except for 13 September. Based on the satellite image of 13 September, the infrared temperature at the ship position was established as −1.2°C, i.e., indicating sea surface temperature. Therefore, this day was a clear-sky case. Only in this case is the vertical structure of relative humidity reproduced relatively well. On the other dates, e.g., 15 September, it was cloudy and, in fact, the infrared temperature derived by the satellite was −2.7°C, which corresponded to the cloud-top temperature. However, the height at which the air temperature was equal to −2.7°C is near the surface (i.e., fog or stratus clouds), while in ERA-I, the cloud top is around 200 hPa because of the saturated condition at the upper troposphere. The vertical structure of specific humidity indicated that the difference was very small compared with relative humidity (not shown), suggesting there might be some problems in the parameterizations of relative humidity and cloud formation in ERA-I.

Ozone partial pressure is completely data-assimilation free in ERA-I. Therefore, it is worth comparing the ERA-I ozone profiles with our observations to assess the performance of ERA-I. Even though our ozone data were not transferred to the GTS, the vertical profiles are reproduced to some extent (Fig. 5). In the troposphere, the observed ozone partial pressure decreases slightly from the surface to the tropopause, while in the lower stratosphere, the value increases up to around 70 hPa. Here, we focus on upper-tropospheric ozone. The typical observed value between 300 and 200 hPa is approximately 2.0 mPa, which is the minimum value in each profile. However, most ERA-I profiles overestimate it by about 0.5 mPa near the tropopause. In other words, the ERA-I vertical gradient of ozone partial pressure is weaker than observed, suggesting that certain mixing processes must be active. One possibility comes from the overestimation of upper-layer cloud and the resultant cloud-top cooling which enhances the vertical mixing processes.

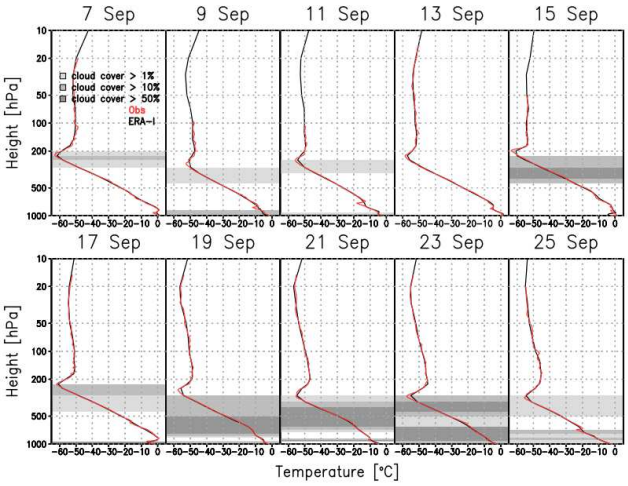

Fig. 3 Vertical profiles of air temperature based on ozonesonde data from *RV Mirai* (red line) and ERA-I values averaged over the two grids closest to the ship (black line) for each day. Gray shading indicates cloud cover in ERA-I (light gray: >1%, medium gray: >10%, dark gray: >50%).

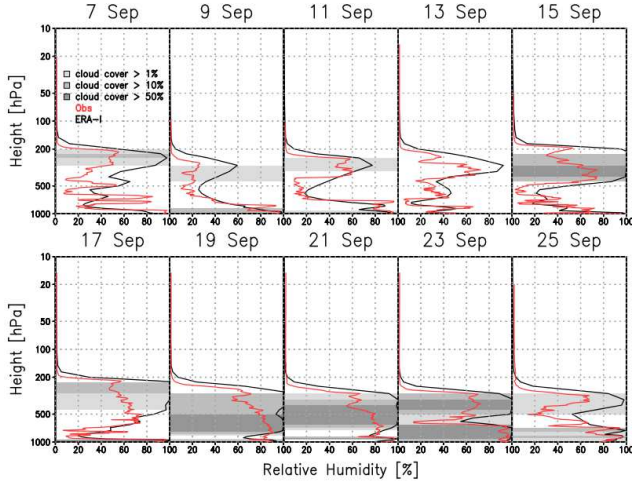

Fig. 4 As in Fig. 3 but for relative humidity.

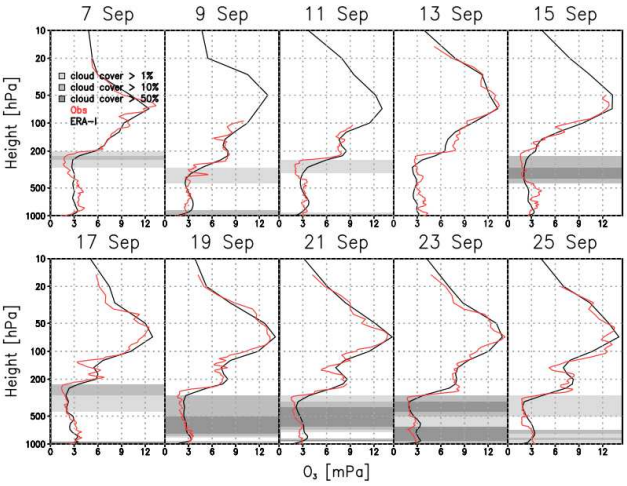

Fig. 5 As in Fig. 3 but for ozone partial pressure.

3.2 Parameterization of cloud and relative humidity in ERA-Interim

Generally, the performance of ERA-I is known as the best among the available reanalysis products, particularly in polar regions (e.g., Inoue *et al.*, 2011; Nicolas and Bromwich, 2011; Lindsay *et al.*, 2014). There have been many development points in ERA-I. One of the remarkable modifications is a new cloud parameterization based on Tompkins *et al.* (2007), which accounts for supersaturation with respect to ice in the cloud-free part of a grid box at temperatures <250 K (Dee *et al.*, 2011). Although they stated that this parameterization leads to substantial increase of relative humidity in the upper troposphere, methods to verify this parameterization are not available because of the bias of the relative humidity data obtained by radiosondes in the upper layers (e.g., Kawai et al., 2017). Nevertheless, the time–height cross sections of relative humidity, illustrated in Fig. 6, clearly show that ERA-I overestimates relative humidity throughout the entire period, particularly between the mid- and upper troposphere. As confirmed from the satellite imagery (Fig. 1; bottom), upper clouds were absent on 15 September, while ERA-I appears to have a thick cloud layer from 500 to 200 hPa (Fig. 7; top).

Following the implementation of a new moist boundary layer scheme in ERA-I (Köhler *et al.*, 2005; Köhler *et al.*, 2011), it was reported that marine cloud cover increased by 15%–25%, even over the Arctic Ocean (Dee *et al.*, 2011). This is partly consistent with our results shown in Fig. 7 (i.e., overestimation of cloud cover in the upper troposphere under cold conditions with temperatures <250 K). Time series of the downward shortwave and longwave radiation derived from the observations and ERA-I indicate that the overestimated upper-layer clouds sometimes affect the negative (positive) bias in shortwave (longwave) radiation (Fig. 7). For example, on 15 September (Figs. 1 and 2), the shortwave and longwave radiation was underestimated by more than 50 W m^{-2} and overestimated by more 20 W m^{-2}, respectively, in ERA-I. The converse situation was observed on 7 September mainly because of the lack of low-level clouds (see relative humidity in Fig. 6).

As reported by Dee *et al.* (2011), the entrainment process at the top of the boundary layer for the moist boundary layer is explicitly prescribed in terms of buoyancy flux with a surface buoyancy component (Troen and Mahrt, 1986; Holtslag, 1998) and a cloud-top radiative cooling component (Lock, 1998). Therefore, once upper-tropospheric clouds are formed, these buoyancy-driven mixing processes

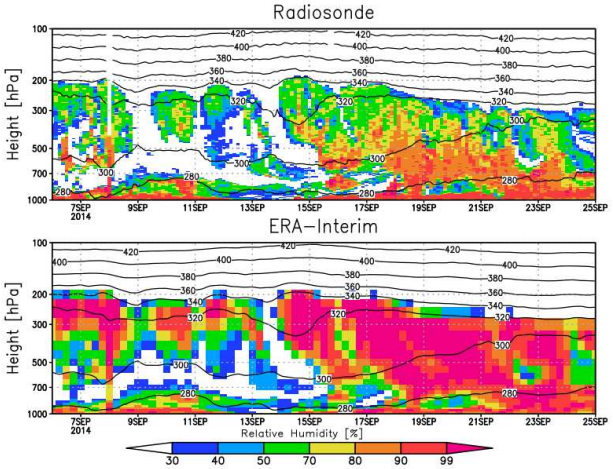

Fig. 6 Time–height cross sections of relative humidity (%: shading) and potential temperature (K: contours) based on observations (upper) and ERA-I

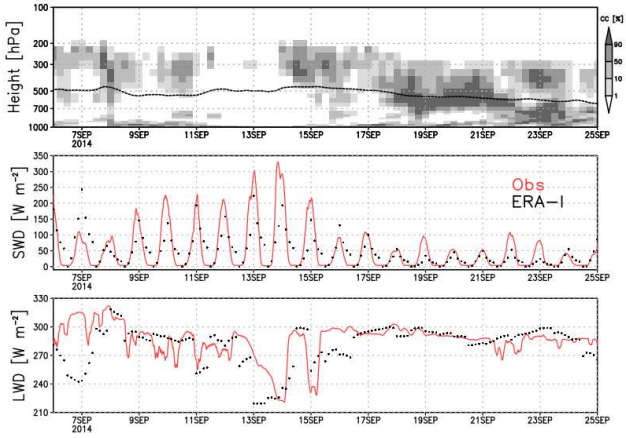

Fig. 7 Time–height cross sections of cloud cover in ERA-I (upper), and downward shortwave (middle) and longwave (lower) radiation based on observations (red line) and ERA-I (black dots). Black contour indicates air temperature of 250 K. Observed values are 3-h running means.

start. When the mass flux term is used to calculate the counter-gradient transport at the top of the overestimated clouds, additional biases would be expected in ERA-I. Here, we focus on the ozone partial pressure and relative humidity near the tropopause. If entrainment of a dry air mass with high ozone partial pressure were active from the lower stratosphere into the upper troposphere, because of evaporative and radiative cooling at the cloud top, the high-ozone air mass would be transported into the upper troposphere, whereas the moist air would be transported into the lower stratosphere. In fact, the ozone partial pressure in ERA-I is larger than observed, particularly for cloudy cases near the tropopause (Fig. 5). In addition, the relative humidity is overestimated in ERA-I above the tropopause, indicating that a small amount

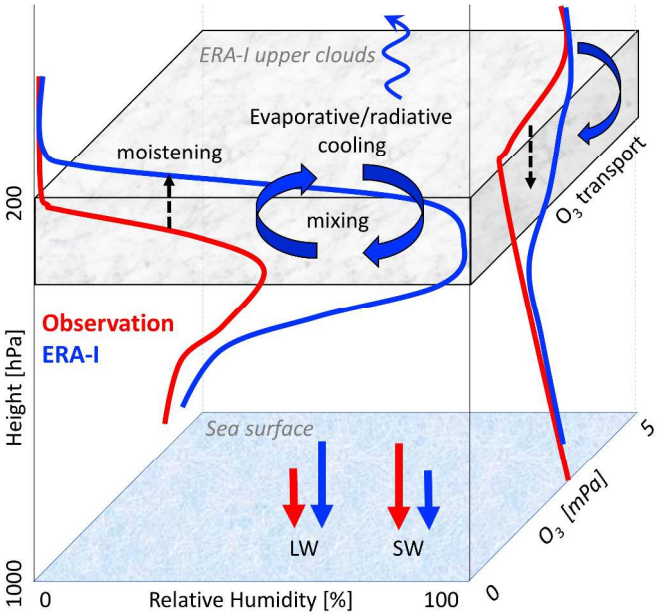

Fig. 8 Schematic of processes in ERA-I associated with overestimated upper-layer cloud (gray box). Red (blue) arrows and lines indicate the observed (ERA-I) situation of surface radiation and profiles of relative humidity and ozone partial pressure.

of moisture has been transported into the lower troposphere (Fig. 4).

In the real condition, based on our observations, relative humidity at the mid- and upper troposphere is relatively low; thus upper tropospheric clouds and evidences of mixing processes across the tropopause were not remarkable.

4. CONCLUSION

Using a tracer of ozone partial pressure, obtained by the ozonesondes launched from the *RV Mirai* over the Arctic Ocean, the ERA-Interim reanalysis product was evaluated by focusing on the mixing at the cloud top, moistening of the lower stratosphere, and surface radiation balance. A schematic summarizing the processes discussed in this study is illustrated in Fig. 8. Compared with the observations, excessive upper-tropospheric clouds were found in ERA-I because of conditions favorable for cloud formation. The ozone partial pressure near the tropopause was larger than observed, suggesting the downward transport of a high-ozone air mass across the tropopause via entrainment. Such a mixing process was also found in the relative humidity field with a moist bias in the lower stratosphere. These mixing processes would be caused by radiative/evaporative cooling at the cloud top. The overestimation of clouds in ERA-I also resulted in disagreement in the surface radiation balance in the case of absent low-level boundary layer clouds. Under ongoing Arctic amplification, the condition of humidity and the cloud condition at upper troposphere would be expected to become more important in understanding the radiation balance at the surface as well as at the top of the atmosphere. This study did not investigate the seasonal variability of the reproducibility of the ERA-Interim reanalysis product; however, a full years' special observations (e.g., Year of Polar Prediction: http://www.polarprediction.net/yopp-activities/; MOSAiC: http://www.mosaic observatory.org/) would make such an evaluation possible in the near future.

ACKNOWLEDGMENTS

We thank the crew of the *R/V Mirai* and all the scientists who supported the observations. This work was supported by a Grant-in-Aid for Scientific Research (KAKENHI(A) 24241009) and the Arctic Challenge for Sustainability (ArCS) project. We thank James Buxton MSc from Edanz Group (www.edanzediting.com./ac) for editing a draft of this manuscript.

REFERENCES

Curry, J. A. and A. H. Lynch (2002): Comparing Arctic regional climate models. *EOS Trans. AGU*, **83**, 87.

Curry, J. A. and 26 others (2000): FIRE Arctic clouds experiment. *Bull. Amer. Meteorol. Soc.*, **81**, 5–29.

Dee, D. P. and 35 others (2011): The ERA-Interim reanalysis: configuration and performance of the data assimilation system. *Quart. J. Roy. Meteorol. Soc.*, **137**, 553–597.

ECMWF (2014): ECMWF global data monitoring report September 2014. *ECMWF*. Available at https://www.ecmwf.int/sites/default/files/mmr_201409.pdf.

Holtslag, A. A. M. (1998): Modelling of atmospheric boundary layers. In *Clear and cloudy boundary layers*. Holtslag, A. A. M. and P. Duynkerke, Eds., Royal Netherlands Academy of Arts and Sciences, 85–110.

Inoue, J. (2014): RV Mirai cruise report (MR14-05). *Japan Agency for Marine-Earth Science and Technology, Yokosuka, Japan*. Available at http://www.godac.jamstec.go.jp/catalog/data/doc_catalog/media/MR14-05_all.pdf.

Inoue, J., B. Kosović and J. A. Curry (2005): Evolution of a storm-driven cloudy boundary layer in the Arctic. *Bound.-Layer Meteorol.*, **117**, 213–230.

Inoue, J., J. Liu, J. O. Pinto and J. A. Curry (2006): Intercomparison of Arctic regional climate models: Modeling clouds and radiation for SHEBA in May 1998. *J. Clim.*, 19, 4167–4178.

Inoue, J., M. E. Hori, T. Enomoto and T. Kikuchi (2011): Intercomparison of surface heat transfer near the Arctic marginal ice zone for multiple reanalyses: A case study of September 2009. *SOLA*, **7**, 57–60.

Intrieri, J. M., M. D. Shupe, T. Uttal and B. J. McCarty (2002): An annual cycle of Arctic cloud characteristics observed by radar and lidar at SHEBA. *J. Geophys. Res.*, **107(C10)**, 8030.

Kawai, Y., M. Katsumata, K. Oshima, M. E. Hori and J. Inoue (2017): Comparison of Vaisala radiosondes RS41 and RS92 in the oceans ranging from the Arctic to tropics. *Atm. Meas. Tech.*, **10**, 2485–2498.

Köhler, M. (2005): Improved prediction of boundary layer clouds. *ECMWF Newsletter*, **104**, 18–22.

Köhler, M., M. Ahlgrimm and A. Beljaars (2011): Unified treatment of dry convective and stratocumulus-topped boundary layers in the ECMWF model. *Quart. J. Roy. Meteorol. Soc.*, **137**, 43–57.

Lindsay, R., W. Wensnahan, A. Schweiger and J. Zhang (2014): Evaluation of seven different atmospheric reanalysis products in the Arctic. *J. Clim.*, **27**, 2588–2606.

Liu, Y. and J. R. Key (2016): Assessment of Arctic cloud cover anomalies in atmospheric reanalysis products using satellite data. *J. Clim.*, **29**, 6065–6083.

Lock, A. P. (1998): The parameterization of entrainment in cloudy boundary layers. *Quart. J. Roy. Meteorol. Soc.*, **124**, 2729–2753.

Maturilli, M. and M. Kayser (2016): Arctic warming, moisture increase and circulation changes observed in the Ny-Ålesund homogenized radiosonde record. *Theor. Appl. Clim.*, doi:10.1007/s00704-016-1864-0.

Nicholls, S. and J. Leighton (1986): An observational study of the structure of stratiform cloud sheets: Part I. structure. *Quart. J. Roy. Meteorol. Soc.*, **112**, 431–460.

Nicolas, J. P. and D. H. Bromwich (2011): New reconstruction of Antarctic near-surface temperatures: Multidecadal trends and reliability of global reanalyses. *J. Clim.*, **27**, 8070–8093.

Sato, K., J. Inoue, Y.-M. Kodama and J. E. Overland (2012): Impact of Arctic sea-ice retreat on the recent change in cloud-base height during autumn. *Geophys. Res. Lett.*, **39**, L10503.

Schweiger, A. J., R. W. Lindsay, S. Vavrus, and J. A. Francis (2008): Relationships between Arctic sea ice and clouds during autumn. *J. Clim.*, **2**1, 4799–4810.

Tjernström, M., J. Sedlar, and M. D. Shupe (2008): How well do regional climate models reproduce radiation and clouds in the Arctic? An evaluation of ARCMIP simulations. *J. Appl. Meteorol. Climatol.*, **47**, 2405–2422.

Tompkins, A. M., K. Gierens and G. Rädel (2007): Ice supersaturation in the ECMWF integrated forecast system. *Quart. J. Roy. Meteorol. Soc.*, **133**, 53–63.

Troen, I. B. and L. Mahrt (1986): A simple model of the atmospheric boundary layer; Sensitivity to surface evaporation. *Bound.-Layer Meteorol.*, **37**, 129–148.

Uttal, T. and 27 others (2002): Surface heat budget of Arctic Ocean. *Bull. Amer. Meteorol. Soc.*, **83**, 255–275.

Summary in Japanese

和文要約

北極海上の気象観測データを用いた ERA-Interim 大気再解析プロダクトの対流圏上部の再現性

猪上淳[1]，佐藤和敏[2]，大島和裕[3]

[1]国立極地研究所, [2]タスマニア大学, [3]海洋研究開発機構

海洋地球研究船「みらい」を用いた北極海での約 3 週間にわたる定点観測を2014年9月に実施した．3時間毎のラジオゾンデ観測，2日毎のオゾンゾンデ観測，連続海上気象観測によるデータを用い，ERA-Interim 再解析プロダクトの再現性を評価した．気温・オゾン分圧・相対湿度の鉛直分布を比較したところ，気温の再現性が高いのに対し，相対湿度は対流圏中層から上部，および成層圏下部において 20%～40%過大評価，オゾン分圧は対流圏界面直下で 0.5mPa 過大評価していた．相対湿度の時間高度断面を比較すると，期間を通じて対流圏上部を中心に明瞭な湿潤バイアスが存在し，雲量も過大評価される傾向にあった．これは気温 250K よりも低温状態で活性化する ERA-Interim 内の雲生成のパラメタリゼーションが主要因であると示唆される．雲頂部の放射・蒸発冷却による混合過程は，成層圏下部からの高オゾン気塊のエントレインメント（下方輸送），および対流圏上部の湿潤気塊の上方輸送を促すと考えられ，観測結果ともとも整合的であった．上層雲のバイアスは海面放射バランスにも影響を与え，特に下層雲を伴わない場合に顕著に現れた．